

Redox Reactions Associated with Iron Release from Mammalian Ferritin[†]D. L. Jacobs,[‡] G. D. Watt,* R. B. Frankel,[§] and G. C. Papaefthymiou^{||}

Department of Physics, California Polytechnic University, San Luis Obispo, California 93407, Francis Bitter National Magnet Laboratory, Massachusetts Institute of Technology, Cambridge, Massachusetts 02139, Department of Chemistry and Biochemistry, University of Colorado, Boulder, Colorado 80309-0215, and Battelle Memorial Institute, Columbus, Ohio 43201

Received June 30, 1988; Revised Manuscript Received September 1, 1988

ABSTRACT: The early redox events involved in iron reduction and mobilization in mammalian ferritin have been investigated by several techniques. Sedimentation velocity measurements of ferritin samples with altered core sizes, prepared by partial reduction and Fe^{2+} chelation, suggest two different events occur during iron loss from the ferritin core. Reductive optical titrations confirm this biphasic behavior by showing that the first 20–30% of core reduction has different optical properties than the latter 70–80%. Proton uptake during initial core reduction is near zero, but as the percent core reduction increases, the proton uptake (H^+/e) values increase to 2 H^+/e (2 $\text{H}^+/\text{Fe}^{3+}$ reduced) as core reduction approaches 1 e/Fe^{3+} . Coulometric reduction of ferritin by mediators of different redox potential and different cross-sectional areas show a two-phase sigmoidal reaction pattern in which initial core reduction occurs at a slower rate than later core reduction. The above experiments were all conducted in the absence of iron chelators so that the observed results were all attributed to core reduction rather than the combined effects of core reduction accompanied by Fe^{2+} chelation. The coulometric reduction of ferritin by various mediators shows a correlation more with reduction potential than with molecular cross-sectional area. The role of the ferritin channels in core reduction is considered in terms of the reported results.

Mammalian ferritin is a hollow, spherical protein molecule consisting of 24 subunits (Ford et al., 1984) which sequesters large amounts of iron as an oxo-hydroxy iron mineral in the protein interior. This protein performs the two important specific biological functions of storing excess cellular iron and releasing it to cellular processes as needed [see Aisen and Listowsky (1980), Crichton and Charleaux-Wauters (1987), and Theil (1987) for reviews]. These two functions are nearly diametrically opposed, however, in terms of the conditions required for their *in vitro* expression. For example, the deposition of Fe^{3+} into the core requires the presentation of Fe^{2+} to apo- or holo-ferritin under the moderately strong oxidizing conditions provided by O_2 or IO_3^- (Macara et al., 1972; Bryce & Crichton, 1973), whereas iron release is accomplished by the anaerobic reaction of ferritin with moderately strong reducing agents (thiols, FMNH₂) with redox potentials more negative than ~ -200 mV at pH 7.0 (Sirivich et al., 1974; Jones et al., 1978). Recent evidence suggests (Watt et al., 1985, 1986) that iron chelators are also essential to the iron release process, because fully reduced mammalian and bacterial ferritins are quite stable with respect to Fe^{2+} loss in the absence of iron complexing agents.

The protein shell of ferritin is clearly permeable to iron which can be readily added to or removed from the protein interior under the appropriate redox conditions. The transfer of other molecules such as O_2 , reductants, and perhaps iron chelators through the protein shell is implicated (Macara et al., 1972; Bryce & Crichton, 1973) by a number of kinetic

experiments of iron deposition ($\text{Fe}^{2+} + \text{O}_2$ or $\text{IO}_3^-/\text{S}_2\text{O}_3^{2-}$) or release (reducing agents + chelators) (Sirivech et al., 1974; Jones et al., 1978). The suggested permeability of the protein shell arises from naturally occurring channels collinear with 3-fold and 4-fold molecular symmetry axes formed where subunits intersect (Harrison et al., 1975; Banyard et al., 1978; Ford et al., 1984). The diameters of the larger identical channels in apoferritin were initially determined to be 8–12 Å (Harrison et al., 1975), but later refinements (Rice et al., 1983; Ford et al., 1984) indicate channel diameters nearer 4–5 Å. These dimensions are large enough to accommodate hydrated Fe^{2+} but only marginally accommodating for FMNH₂, FADH₂, bipyridyl, etc. These latter molecules are thought (Jones et al., 1978) to participate in the mobilization of iron from the ferritin mineral core by (1) diffusion through the channels into the protein interior, (2) undergoing redox reactions with the surface Fe^{3+} ions of the mineral core forming Fe^{2+} , and (3) subsequent removal of the resulting Fe^{2+} by chelating agents. This proposed mechanism implies a “last in first out” sequence for the iron flux in ferritin, a result consistent with ⁵⁹Fe labeling experiments (Hoy et al., 1974; Treffry & Harrison, 1978) and experiments reported here.

To further examine certain aspects of the mechanism of iron regulation by ferritin, we have studied the redox properties, proton fluxes produced during reduction, and properties of ferritin samples which have been subjected to partial reduction and selective removal of part of the iron-containing core. The results of these studies provide insights into the early events of iron release from the iron-containing core of the ferritin molecule.

MATERIALS AND METHODS

Horse spleen ferritin was obtained from Sigma at a nominal concentration of 100 mg/mL in 0.15 M NaCl. This stock ferritin solution was diluted to the desired working concentrations (10–30 mg/mL) with 0.025 M *N*-[tris(hydroxymethyl)methyl]-2-aminoethanesulfonic acid (TES),¹ and the

[†] This research was supported by National Science Foundation Grant DMB 8512382 from the Biophysics Program and by Contract N0014-86-K-0102 from the Bioelectromagnetics Program of the Office of Naval Research.

* To whom correspondence should be addressed at the University of Colorado.

[‡] Battelle Memorial Institute.

[§] California Polytechnic University.

^{||} Massachusetts Institute of Technology.

protein (Lowry) and iron (Lovenberg et al., 1963) concentrations were determined. Total iron was determined to be 2100 iron atoms per ferritin molecule. Apoferritin was prepared by the thioglycolic acid dialysis of holoferritin (Treffry & Harrison, 1978) and total protein determined by the Lowry method.

Ferritin samples having 10%, 20%, 30%, 40%, 60%, 80%, and 100% of the original 2100 Fe^{3+} ferritin removed were prepared anaerobically by (1) reducing ferritin to the desired extent (i.e., 20%, 40%, etc.) with $\text{S}_2\text{O}_4^{2-}$ containing 5×10^{-5} M methylviologen (MV) for 30 min, (2) adding excess bipyridyl (bipyd) and incubating an additional 30 min, and (3) separating $\text{Fe}(\text{bipyd})_3^{2+}$ from ferritin on an anaerobic 1×40 cm, G-25 Sephadex column equilibrated in 0.025 M TES/0.1 M NaCl, pH 7.5. The emerging ferritin was free of $\text{Fe}(\text{bipyd})_3^{2+}$, and the ferritin-bound iron was all in the Fe^{3+} state, as determined by coulometry (Watt, 1979) and Mossbauer spectroscopy. These modified ferritin samples were concentrated, their protein concentrations were determined by the Lowry method, and their iron content was determined (Lovenberg et al., 1963). Sedimentation patterns for each protein sample (10 mg/mL in 0.05 M TES/0.1 M NaCl, pH 7.5) were recorded on a Beckman Model E ultracentrifuge under identical ultracentrifugation conditions of 50 400 rpm and 20 °C.

Proton uptake by ferritin during core reduction was measured with stirred 1.0-mL samples (0.1 mg/mL, 0.5 mM in Fe^{3+}) which had been dialyzed against several changes of 0.15 M NaCl to remove small molecule buffering components. The pH was first adjusted with 0.01 M NaOH to the desired pH in a Vacuum Atmospheres glovebox (<1.0 ppm O_2), followed by 25- μL additions of 1×10^{-3} M reduced MV. After each MV addition, standardized 0.005 M HCl was used to adjust the pH back to its original value and to quantitate the proton exchange occurring upon reduction. Several additions of MV were made to the same ferritin sample until the latter became 10–40% reduced (depending on the pH) after which MV is no longer a stoichiometric reductant due to the back-potential resulting from oxidized MV buildup. The advantage of using MV is that it is a low-potential reductant whose redox reaction is pH independent, and, therefore, the measured proton stoichiometry is attributable directly to ferritin reactions.

Optical titrations of ferritin, containing 1×10^{-5} M MV as mediator, with standardized aliquots of $\text{S}_2\text{O}_4^{2-}$ were conducted in anaerobic 1-mL quartz cells and monitored in the 350–800-nm range. The quartz cells were filled and sealed in the glovebox, and additions were made through a septum–stopcock combination, the latter sealing the cell contents from the atmosphere after $\text{S}_2\text{O}_4^{2-}$ addition through the septum. Electrophoresis measurements of Fe^{3+} –holo-, apo-, and Fe^{2+} –holoferritin were run in a Vacuum Atmosphere glovebox to prevent Fe^{2+} –holo oxidation using a GE-4 Pharmacia gel electrophoresis apparatus. The gels were prerun for 30 min with 1.0 mM $\text{S}_2\text{O}_4^{2-}$ prior to sample loading to further ensure anaerobic conditions, and then the samples (10–30 μg) were run at a constant current of 20 mA for 1.5 h. The gels were stained with Coomassie Blue and the protein migration rates compared.

Mediated, electrochemical reduction of ferritin was conducted as previously described (Watt et al., 1985) using FMN, phenosafranine, neutral red, and various substituted viologens as mediators at 1×10^{-4} M at pH 8.0. The current flow in

microamperes (microcoulombs per second) is a direct measure of the rate of ferritin reduction by the mediator and was used to assess the relative reduction rates of the mediators investigated.

The diffusion of FMN, bipyd, MV, and BV into the interior of apo- and holoferritin was studied by (1) incubating anaerobically one of the above molecules at 1×10^{-3} M with 1–2 mL of either apo- or holoferritin (~ 15 mg/mL) for periods of time ranging from several days to 2 weeks and (2) separating the larger ferritin from the added small molecule by rapid passage (1–2 min) through an anaerobic Sephadex G-25 column. The analysis for the added small molecules in the emerging ferritin fraction was carried out by (1) optical and fluorescence methods for FMN, (2) the anaerobic addition of Fe^{2+} and subsequent colorimetric analysis of the mixture for $\text{Fe}(\text{bipyd})_3^{2+}$, and (3) addition of $\text{S}_2\text{O}_4^{2-}$ to the ferritin fraction and analysis for the free radical form of MV $^{\cdot}$ and BV $^{\cdot}$ by low-temperature electron paramagnetic resonance (EPR) spectroscopy.

RESULTS

Sedimentation Measurements. The removal of Fe from the ferritin core in desired increments is easily accomplished experimentally by fractional reduction of the core iron followed by chelation and removal of the resulting Fe^{2+} . Separation of the chelated Fe^{2+} from ferritin by G-25 Sephadex chromatography provides Fe^{3+} –ferritin samples in which selected amounts of iron have been removed from the mineral cores. However, since the original ferritin is heterogeneous (i.e., contained a distribution of molecules with different core sizes), the question arises whether the iron removal step is uniform (a constant percentage of the iron is removed from each molecule of the molecular distribution) or nonuniform (a greater loss from specific components of the distribution, such as from the lightly or heavily loaded molecules). We have used ultracentrifugation methods to compare sedimentation velocities of ferritin samples which have had their iron content altered by fractional reduction followed by Fe^{2+} removal by chelation. Starting with ferritin whose average core size is 2100 iron atoms and removing iron in 10–20% increments (10% increments for 0–40% iron loss; 20% increments for 40–100% iron loss), the molecular mass changes by $(2100)(0.2)(89) = 37\,400$ daltons for each 20% iron loss increment. This change in molecular mass is sufficient to measure by ultracentrifugation methods. In this calculation, we assume an FeOOH unit ($M_r = 89$) is lost for each Fe^{2+} removed by reduction and chelation.

In Figure 1 is a series of sedimentation patterns resulting from ferritin samples of identical protein concentration but whose iron contents have been decreased by 20% increments (the 10% and 30% iron loss samples are not shown). The original sample is seen to be a heterogeneous mixture of ferritin molecules ranging from those rapidly sedimenting (heavily filled cores) on the right to apoferritin shown as the “spike” on the left. The individual patterns are all aligned at the apo spike, and a vertical line is drawn from the peak of the iron core distribution in the native sample through each of the remaining patterns. All curves in Figure 1 were obtained at the same protein concentrations and ultracentrifuge conditions and are directly comparable. Qualitatively, there are several changes seen in the sedimentation patterns. Initial iron loss seems to occur essentially uniformly because the peak position remains constant but the overall distribution curve tends to flatten (compare 0% and 20% curves). A noticeable rise in the apo peak occurs with this initial iron loss, indicating the conversion of some of the lightly loaded molecules into apo-

¹ Abbreviations: MV, methylviologen; BV, benzylviologen; bipyd, 2,2'-bipyridine; TES, *N*-[tris(hydroxymethyl)methyl]-2-aminoethanesulfonic acid.

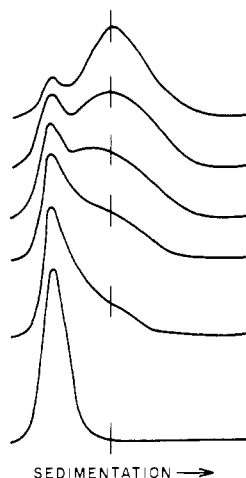


FIGURE 1: Sedimentation patterns of ferritins with altered core sizes. Mammalian ferritin initially containing 2100 Fe^{3+} /molecule was treated to remove iron in 20% increments (see Materials and Methods) and subjected to sedimentation velocity analysis. Sedimentation at 10 mg/mL and 50 400 rpm, corresponding to 100%, 80%, 60%, 40%, 20%, and 0% of the original 2100 Fe, is shown (top to bottom). The direction of increasing centrifugal field is shown by the arrow along the abscissa, and the ferritin concentration gradient is the ordinate.

ferritin. Beginning with the 40% iron loss sample, the peak position moves slightly to the left as do the wings on the high molecular weight side, suggesting a slightly higher rate of iron loss from the heavier components of the distribution. Subsequent iron loss then diminishes the concentration of iron-containing ferritin molecules until eventually only apoferritin remains. The overall qualitative trend of our results appears to be an initial uniform loss of iron from all molecules followed by a more preferential loss of iron from the heavier filled molecules.

Optical Titration. Reductive titrations of ferritin are relevant to the iron release mechanism because they represent the redox reaction which first occurs in the iron core preparatory to iron release from ferritin. In Figure 2a are optical spectra resulting from stepwise reduction of ferritin by standardized $\text{S}_2\text{O}_4^{2-}$ in the presence of 1×10^{-5} M MV as mediator. Identical spectra are obtained in the absence of the MV mediator, but longer reaction times are required for the nonmediated $\text{S}_2\text{O}_4^{2-}$ reduction reaction to occur. Two effects are seen in Figure 2a: (1) an overall decrease in absorbance in the 300–550-nm range and (2) an increase in absorbance at 550–800 nm, but only during the initial stages of reduction. An isosbestic forms at 550 nm during this initial reduction. Figure 2b displays the absorbance changes at 425 and 750 nm in greater detail during the titration. A two-phase reaction is observed in which the absorbance at 750 nm rises until 25–30% of the Fe^{3+} present in the core is reduced, after which the absorbance remains constant during reduction of the remaining Fe^{3+} . At 425 nm, a composite curve consisting of two distinct slopes is seen, the first accounting for 25–30% of the reducing equivalents required to reduce the core iron in ferritin and the second resulting from final reduction of the ferritin core. We have verified that the increase in absorbance in the 580–800-nm range is a result of ferritin core reduction, and not a result of SO_3^{2-} (a product of $\text{S}_2\text{O}_4^{2-}$ oxidation) interaction at the core, by titrating ferritin with electrolytically reduced MV (no $\text{S}_2\text{O}_4^{2-}$ present) and observing the same change at 580–800 nm. Two spectroscopically distinct iron populations are present in ferritin, occurring in a $\sim 1:3.5$ ratio.

Proton Uptake. The anaerobic reaction of reduced MV with ferritin is rapid, and during the early stages of reaction, reduction is accompanied by only small pH increases. However,

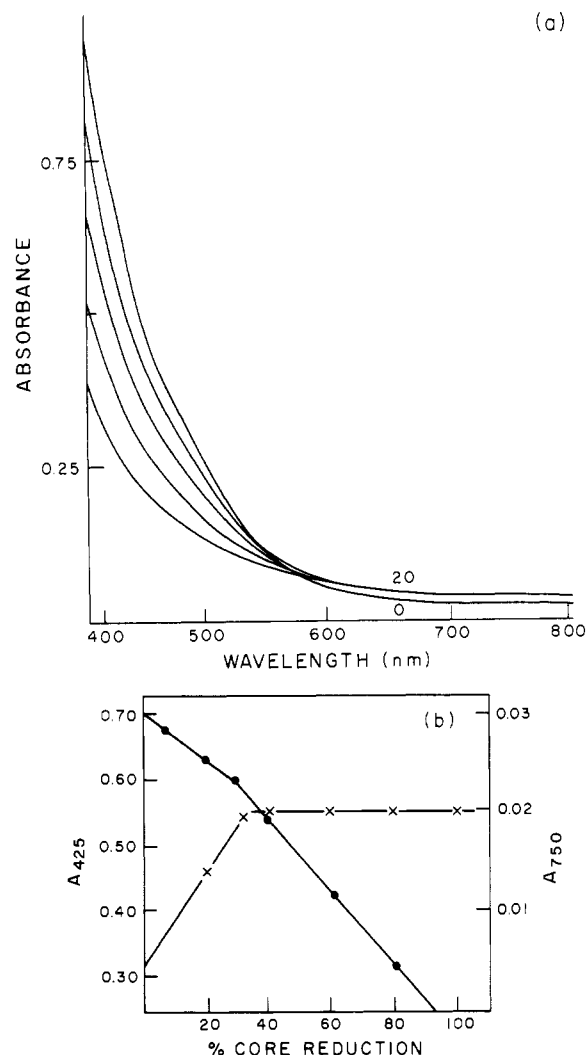


FIGURE 2: Reductive titration of mammalian ferritin. (a) Optical spectra of mammalian ferritin (2100 Fe^{3+} /ferritin) resulting from additions of standardized $\text{S}_2\text{O}_4^{2-}$ (top to bottom). At 750 nm, the 0% and >20% ferritin reduction curves are indicated. (b) Optical titration of ferritin reduction with $\text{S}_2\text{O}_4^{2-}$ at 425 nm (\bullet) and 750 nm (\times).

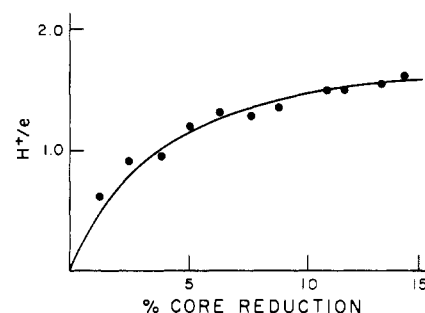


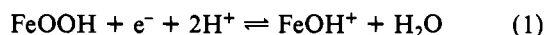
FIGURE 3: Proton uptake during ferritin reduction. The protons taken up per added electron (H^+/e) values as a function of mammalian ferritin core reduction. Ferritin (1 mL of 0.1 mg/mL containing 0.47 mM Fe^{3+}) was reacted at pH 8.0 with 25 μL of 1.05 mM reduced MV. Values of H^+/e were determined from the volume of standardized 5 mM HCl required to return the pH to 8.0 after the MV reaction.

as the extent of ferritin reduction increases, the corresponding pH change increases until eventually a limiting H^+/e value² near 2.0 is reached. Figure 3 shows in detail the proton uptake

² The pH increase could arise either from proton uptake or from hydroxide ion release by the ferritin core during reduction. In what follows, we present and discuss our results in terms of proton uptake.

at pH 8.0 during the initial 15% reduction of ferritin. The reduction at other pH values displayed similar behavior of low H^+/e values at the early stages of reduction, but this ratio increased with increasing reduction, reaching a final limiting value. The numerical H^+/e values obtained as a function of pH were 2.27, 2.14, and 1.6, respectively, at pH 6.0, 7.0, and 8.0. Because the reduction potential of the ferritin core is pH dependent (the core becomes more difficult to reduce with increasing pH) and because the reduction capacity is so large (~ 2100 MV, are required to reduce each ferritin molecule), the MV reductant is effective in reducing ferritin to only a limited degree at higher pH values, and consequently, only low H^+/e values <1.5 are obtained above pH 8.5. At pH 8.0, a value of 2.0 H^+/e is predicted from the variation of the reduction potential with pH (Watt et al., 1985), but because of the effect just discussed, a value of only 1.6 H^+/e was measured directly as shown in Figure 3.

Assuming that the bulk core of the ferritin molecule is electrically neutral and has the composition $FeOOH$, the values near 2.0 for the H^+/e stoichiometry for core reduction suggest that the following reaction occurs during the reduction step:



We have previously shown (Watt et al., 1985, 1986) that in the absence of chelators, the reduced core of ferritin is stable to iron loss. Given these results, it appears that a large positive charge buildup occurs in the reduced ferritin core as reduction proceeds, unless some charge compensation process accompanies the reduction step.

We have compared the electrophoresis patterns of apo-ferritin, holo- Fe^{3+} -ferritin, and holo- Fe^{2+} -ferritin with regard to their electrophoretic mobility on 5% polyacrylamide gels and find identical migration rates for all three species. These results demonstrate that all three ferritin species possess the same overall charge and suggest that anion migration into the core or on to the protein shell occurs during reduction, thereby controlling the charge buildup predicted by eq 1.

Electrochemical Reduction. The coulometric reduction of ferritin, at a fixed concentration of reductant [maintained constant by rapid electrochemical reduction (Watt, 1979)], provides a means for comparing the effectiveness of various reductant molecules toward Fe^{3+} core reduction. Under these zero-order rate conditions, with respect to reductant, the reaction rate depends only upon the reaction characteristics of the ferritin core and the reductant under study. Figure 4 consists of three coulometric reduction curves at pH 8.0 resulting from MV-, BV-, and FMN-mediated, electrochemical reduction of ferritin. The area under the curves represents the total reducing equivalents required for ferritin reduction, and the current, at a given time, represents the rate of electron transfer to the core. Several significant core reactivity features emerge from analysis of Figure 4. Using the current at the peak of each curve as a measure of the maximum rate at which the given reductant reacts with the Fe^{3+} core, it is clear that MV is the superior reductant, reacting 2.3 and 5.4 times faster than BV and FMN, respectively. The rounding of the curves is indicative that the reduction of the Fe^{3+} core is not uniform but consists of a slower initial reaction that either accelerates with time or gives way to a second, faster reaction. The inset in Figure 4 for the BV-mediated reduction reaction was obtained by integrating the middle curve as a function of increasing time. This procedure allows the rate of core reduction to be determined as a function of time under zero-order reductant conditions. The curve is clearly sigmoidal, confirming a nonuniform (biphasic) rate of core reduction. A similar sigmoidal curve was obtained by Jones et al. (1978) for the

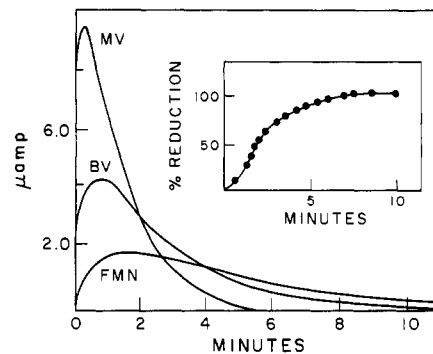


FIGURE 4: Coulometric reduction of mammalian ferritin. The reduction of $10 \mu L$ of mammalian ferritin containing $0.015 M Fe^{3+}$ by controlled potential microcoulometry at pH 8.0 and -500 mV vs NHE using MV (top), BV (middle), and FMN (bottom) as mediators at $7.5 \times 10^{-5} M$ in 0.05 Tris/ $0.25 M$ NaCl. The current flow in microamperes at the peak measures the relative rate of ferritin reduction by the indicated mediators. Inset: A reduction progress curve for mammalian ferritin with BV as mediator showing the sigmoidal nature of the core reduction process.

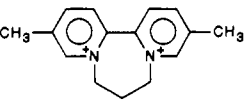
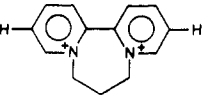
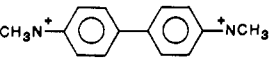
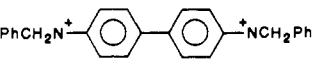
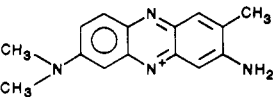
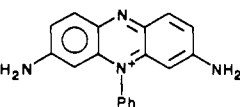
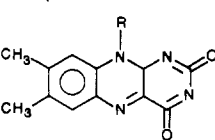
combined reduction and iron release reaction by bipyridyl under zero-order $FMNH_2$ reduction conditions maintained by enzymatic reduction of FMN. Because both reduction of Fe^{3+} and chelation of Fe^{2+} were occurring in the results of Jones et al. (1978), the source of the observed sigmoidicity is not clear. However, Figure 4 indicates that reduction of the core is the step which likely causes the sigmoidal behavior because no significant iron loss occurs under these conditions.

In Table I are listed other redox agents whose reactions with ferritin have been evaluated by the coulometric reduction technique. The reagents studied are essentially planar molecules with the approximate dimensions listed in the table for the two axes describing the molecular plane. With the exception of SO_2^- and BV, all other molecules in Table I are quite similar in their overall dimension, yet the relative reactivity of these reagents differs by a factor of >16 . In the case of BV, the longest dimension of 23 \AA is nearly four times the nominal diameter of the protein channels, and consequently, core reduction by BV via channel penetration would only occur when the long axis of BV is nearly colinear with the channel axis. This steric restriction should severely limit the number of productive BV electron-transfer encounters at the ferritin core and would result in a low BV reactivity. However, BV is found to be a much better reductant than the above argument would predict and to be more effective than the smaller molecules listed below it in Table I. The rate data in Table I, therefore, do not correlate well with molecular dimensions.

A better correlation of ferritin core reduction with reduction potential is evident from the data in Table I. A particularly striking example is seen in the neutral red-phenosafranine comparison where molecules of the same charge type and closely related size and structure differ by over a factor of 3 in Fe^{3+} core reactivity. However, their reactivity difference is consistent with the 75-mV difference in reduction potential. The comparison of neutral red, phenosafranine, and FMN, again molecules of similar overall structure, shows FMN to be inconsistent with the free energy correlation. An explanation for this anomaly may be that FMN is the *in vivo* reductant (Jones et al., 1978) and has a built in recognition specificity that the other two molecules lack, which imparts to FMN a higher reactivity.

The reactivity of $S_2O_4^{2-}$ toward the Fe^{3+} core presents another anomaly with regard to low-potential reductants. In most $S_2O_4^{2-}$ reactions, it is the $SO_2^{\cdot -}$ radical, formed by $S_2O_4^{2-}$

Table I: Properties of Mediators Used for Ferritin Reduction^a

reductant	$E_{1/2}$ (mV)	approximate dimensions (Å)	rel rate
$S_2O_4^{2-}$ (SO ₂ ^{•-}) dithionite	-660	2.0 × 2.0	0.15
	-660	11 × 7.5	1.0
	-540	9.5 × 7.5	1.0
 methylviologen	-440	11 × 4.5	0.95
 benzylviologen	-360	23 × 4.5	0.40
 neutral red	-325	11 × 4.5	0.20
 phenosafranine	-250	10 × 9.0	0.06
 FMN	-215	10 × 6.5	0.17

^aThe mediators used in steady-state electrochemical reduction are ranked in descending order of reduction potential versus NHE at pH 7.0. The approximate molecular dimensions were calculated by assuming planar molecules using the atomic radii of the atoms involved. The relative rate in millimoles of electrons per second transferred to ferritin from the indicated mediator was calculated from the peak current, *i*, in milliamperes from Figure 4 (milliamperes = millicoulombs per second; *i*(milliamperes)/*J*(millicoulombs per millimole of e) = millimoles of e per second; *J* = 96 500 mC/mmol of e is Faraday's constant).

dissociation, which is the active species (Lambeth & Palmer, 1973; Cruetz & Sutin, 1974) with a midpoint potential of -660 mV (Mayhew, 1978). A direct comparison with the reagents in Table I is not possible because SO₃²⁻ (the product of SO₂^{•-} oxidation) is not electroactive at pH 8.0 (Teder, 1973). However, from the reductive and optical titrations of Figure 2, we were able to compare the rate of Fe³⁺ core reduction by S₂O₄²⁻ alone with that of the MV-mediated S₂O₄²⁻ reduction. Under the latter conditions, the rate of Fe³⁺ core reduction is about 5-fold faster than with S₂O₄²⁻, clearly indicating the inferiority of S₂O₄²⁻ compared to MV, even though a favorable 200-mV difference is possessed by S₂O₄²⁻. Molecular size and free energy changes are not factors in this reaction because both strongly favor SO₂^{•-}, which leads us to suggest that the charge difference between SO₂^{•-} and MV_r⁺ (oxidized MV is a dication, and the one-electron-reduced MV_r⁺ is a monocation) is the most important factor in governing their reaction rates with the ferritin core.

Attempts to measure the presence of FMN, bipyd, MV, or BV in the interior of apo- or holoferitin by the methods employed were not successful. The methods used to detect these molecules are sufficiently sensitive that ~0.1 small

molecule per ferritin molecule could have been easily detected. Our results are, therefore, conclusive in showing that no "sluggish" diffusion processes (*t*_{1/2} > 0.5 min) occur involving equilibrium of free small molecules with the ferritin interior via the channels of dimensions near those of the diffusing molecules. However, because of the time scale of our measurements, we are unable to draw any conclusions about facile diffusional processes involving the studied molecules.

DISCUSSION

Most studies involving iron release from the ferritin core have monitored the rate of appearance of Fe²⁺ in chelated form as a function of time, reductant, or other selected conditions. While this is a valid approach for studying overall iron release, it is apparent that this monitored reaction may consist of several separate and definable component reactions such as core reduction, proton transfer, Fe²⁺ chelation, etc. To gain a proper understanding of the mechanism of Fe²⁺ release from ferritin, these component reactions need to be recognized and their characteristics thoroughly and separately delineated. Here, we have examined the reduction of the ferritin core in the absence of the Fe²⁺ chelation reaction and report on the nature of the reduction and attendant proton-transfer reactions.

The ultracentrifugation results in Figure 1, the optical titrations in Figure 2, the proton uptake data of Figure 3, and the coulometric reduction in Figure 4 all show, in varying degrees of detail, that the reduction of the Fe³⁺-containing core consists of two discernible steps. All procedures used for monitoring the reduction reaction have indicated that 20–30% of the Fe³⁺ core behaves differently toward reduction than the remaining 70–80%. Such behavior could result from reduction of a specialized cluster of iron atoms in the core, iron atoms bound to the protein interior surface, or perhaps the reduction of iron atoms forming the outer layers of the mineral surface. Once this initial reaction is completed, our results suggest a measurably greater rate of core reduction and iron loss from the heavier molecules, a result consistent with preferential iron loss from the larger area of more highly filled ferritin cores (Hoy et al., 1974).

The optical titrations in Figure 2 clearly demonstrate the spectral uniqueness of the two types of iron atoms in the ferritin core. Both types possess absorption in the 350–500-nm range, but only the initial 20–30% of the iron atoms that react with reductant display absorbance increases in the 580–800-nm region. Figure 4 shows that this initial reaction is slightly slower than the bulk core reduction, giving rise to the rounding of the reduction curves and the sigmoidicity of the overall core reduction reaction.

The early stages of core reduction occur with little or no accompanying proton uptake, but as reduction increases, proton uptake also increases, reaching a limiting value near 2.0 H⁺/e, a result in keeping with previous studies (Watt et al., 1985). As reaction 1 indicates, a net +1 charge increase occurs for each iron atom reduced which if unchecked could lead to a +2100 charge buildup for complete core reduction. The electrophoresis results of apoferritin, Fe³⁺-holoferritin, and Fe²⁺-holoferritin show that all three samples migrate identically, a result which indicates that all ferritin molecules possess the same charge and that no such charge buildup occurs. From this result, we conclude that anion transfer accompanies electron/proton transfer. At this point, we have no information regarding which anions are involved [the ferritin solutions used in this study contained only the anions of TES buffer (~0.01 M), Cl⁻ (~0.1 M) and, of course, OH⁻] nor their destination of migration, although the mineral core is the most probable site.

The optical titrations, when considered with the proton uptake data, indicate that the initial reduction of the core occurs at a unique set of iron atoms with separate optical properties and redox reactions that do not involve proton exchange. This reaction could occur at the surface of the mineral core, in which case the iron atoms are likely to be in a more protonated or hydrated state relative to those deeper within the core which are likely to be in the FeOOH state. However, an alternative but related view is that this unique group of iron atoms are those attached to the phosphate known to be present in the mammalian ferritin iron core. The observed spectral differences would arise from iron atoms associated with phosphate relative to those bound only to the oxo-hydroxy matrix of the core. The lack of initial proton uptake (Figure 3) is explainable because either the iron atoms are different from those depicted in reaction 1 or the phosphate present acts as a localized buffering agent.

Table I shows that the ferritin core undergoes reduction with a number of different types of reductants at rates which correlate more with redox potential than with molecular size, even though most molecules exceed the nominal diameter of the ferritin channels. We found no evidence that selected molecules in Table I are "trapped" in the ferritin interior by restricted diffusional processes, an effect that might be expected when the molecular dimensions of the diffusant approach the size of the channel through which it is to travel (Sturhman, et al., 1976; Fish, 1976). This negative result allows only the partial and limited conclusions to be drawn that if restricted diffusion is present it occurs faster than our measurement interval or, quite possibly, the molecules never diffuse into the ferritin interior. The latter conclusion is consistent with the results of May and Fish (1977), who report that restricted access to the ferritin interior occurs with molecules much smaller than those in Table I. A similar view was presented by Stuhmann et al. (1976) from neutron diffraction studies. Our results are not definitive enough to confirm these reported results but when taken together with them suggest that alternate mechanisms to deliver electrons to the Fe³⁺ core other than reductant transfer through the channels be explored in further detail. Preliminary results from such studies have been reported (Watt et al., 1988) and indicate that facile electron transfer to the ferritin core occurs with protein redox agents whose large size precludes their entry into the ferritin interior by passage through the ferritin channels. Thus, Watt et al. (1988) suggest that electron transfer to the ferritin core occurs by mediation from channel-bound Fe²⁺ or Fe³⁺ ions or possibly even by electron

tunneling through the protein shell.

Registry No. Fe, 7439-89-6; H⁺, 12408-02-5.

REFERENCES

- Aisen, P., & Listowsky, I. (1980) *Annu. Rev. Biochem.* **49**, 375-393.
- Banyard, S. H., Stammers, D. K., & Harrison, P. M. (1978) *Nature* **271**, 282-284.
- Bryce, C. F. A., & Crichton, R. R. (1973) *Biochem. J.* **133**, 301-309.
- Crichton, R. R. (1973) *Struct. Bonding (Berlin)* **17**, 67-134.
- Cruetz, C., & Sutin, N. (1974) *Inorg. Chem.* **13**, 2041-2043.
- Fish, W. W. (1976) *J. Theor. Biol.* **60**, 385-392.
- Ford, B. C., Harrison, P. M., Rice, D. W., Smith, J. M. S., Treffry, A., White, J. L., & Yariv, J. (1984) *Philos. Trans. R. Soc. London*, **B304**, 551-565.
- Harrison, P. M., Hoy, T. G., & Hoare, R. J. (1975) in *Proteins of Iron Storage and Transport in Biochemistry and Medicine* (Crichton, R. R., Ed.) pp 269-278, Elsevier Inc., New York.
- Hoy, T. G., Harrison, P. M., & Shabbir, M. (1974) *Biochem. J.* **139**, 603-608.
- Jones, T., Spencer, R., & Walsh, C. (1978) *J. Am. Chem. Soc.* **100**, 4011-4018.
- Lambeth, D. O., & Palmer, G. (1973) *J. Biol. Chem.* **248**, 6095-6103.
- Lovenberg, W. M., Buchanan, B. B., & Rabinowitz, J. C. (1963) *J. Biol. Chem.* **238**, 3899-3906.
- Macara, I. G., Hoy, T. G., & Harrison, P. M. (1972) *Biochem. J.* **126**, 151-162.
- Mahew, S. G. (1978) *Eur. J. Biochem.* **85**, 535-547.
- May, P., & Fish, W. W. (1977) in *Proteins of Iron Metabolism* (Brown, E. B., Aisen, P., Fielding, J., & Crichton, R. R., Eds.) pp 31-37, Grune & Straton, New York.
- Sirivech, S., Frieden, E., & Osaki, S. (1974) *Biochem. J.* **143**, 311-315.
- Stuhrman, H. B., Hass, J., Ibel, K., Koch, M. H. J., & Crichton, R. R. (1976) *J. Mol. Biol.* **100**, 399-413.
- Teder, A. (1973) *Acta Chem. Scand.* **27**, 705-731.
- Treffry, A., & Harrison, P. M. (1978) *Biochem. J.* **171**, 313-320.
- Watt, G. D., Frankel, R. B., & Papaefthymiou, G. C. (1985) *Proc. Natl. Acad. Sci. U.S.A.* **82**, 3640-3643.
- Watt, G. D., Frankel, R. B., Papaefthymiou, G. C., Spartalian, K., & Stiefel, E. I. (1986) *Biochemistry* **25**, 4330-4336.
- Watt, G. D., Jacobs, D., & Frankel, R. B. (1988) *Proc. Natl. Acad. Sci. U.S.A.* **85**, 7457-7461.